Journal of Hazardous Materials 313 (2016) 18–28

Contents lists available at ScienceDirect

Journal of Hazardous Materials

journal homepage: www.elsevier.com/locate/jhazmat

Low dose perfluorooctanoate exposure promotes cell proliferation in a human non-tumor liver cell line

Hongxia Zhang[a,1], Ruina Cui[a,1], Xuejiang Guo[b], Jiayue Hu[a], Jiayin Dai[a,*]

[a] Key Laboratory of Animal Ecology and Conservation Biology, Institute of Zoology, Chinese Academy of Sciences, Beijing 100101, PR China
[b] State Key Laboratory of Reproductive Medicine, Nanjing Medical University, Nanjing 210029, PR China

HIGHLIGHTS

- Differential expression of proteins induced by PFOA in HL-7702 was identified.
- Most of the differentially expressed proteins are related to cell proliferation.
- A low dose of PFOA stimulates HL-7702 cell proliferation.
- A high dose of PFOA inhibits HL-7702 cell proliferation.

ARTICLE INFO

Article history:
Received 29 December 2015
Received in revised form 25 March 2016
Accepted 27 March 2016
Available online 29 March 2016

Keywords:
PFOA
iTRAQ
Human cells
Cell proliferation

ABSTRACT

Perfluorooctanoate (PFOA) is a well-known persistent organic pollutant widely found in the environment, wildlife and humans. Medical surveillance and experimental studies have investigated the potential effects of PFOA on human livers, but the hepatotoxicity of PFOA on humans and its underlying mechanism remain to be clarified. We exposed a human liver cell line (HL-7702) to 50 μM PFOA for 48 h and 96 h, and identified 111 significantly differentially expressed proteins by iTRAQ analysis. A total of 46 proteins were related to cell proliferation and apoptosis. Through further analysis of the cell cycle, apoptosis and their related proteins, we found that low doses of PFOA (50–100 μM) promoted cell proliferation and numbers by promoting cells from the G1 to S phases, whereas high doses of PFOA (200–400 μM) led to reduced HL-7702 cell numbers compared with that of the control mainly due to cell cycle arrest in the G0/G1 phase. To our knowledge, this is the first report on the promotion of cell cycle progression in human cells following PFOA exposure.

1. Introduction

Due to their chemical and thermal resistance and ability to repel both oil and water, perfluoroalkyl acids (PFAAs) have been widely used in a variety of industrial and consumer applications over the past 50 years, including surfactants, lubricants, adhesives, paints, fire-fighting foams and cosmetics [1]. Paradoxically, their thermal and chemical persistence also results in a high degree of environmental persistence and bioaccumulation. As a result, PFAAs have been found in the ocean, air, wildlife and humans worldwide [2,3]. Perfluorooctanoate (PFOA) is one of the most often reported and discussed PFAAs in the scientific literatures [3–6]. The population geometric mean for serum PFOA has been reported to be 32.91 ng/mL in districts with PFOA contaminated water [7] which was about 5–8 fold higher than previously reported for a representative American population based on NHANES (National Health and Nutrition Examination Survey) data from 1999 to 2000 and 2007 to 2010, respectively [8,9]. The highest levels of PFOA were described in ammonium perfluorooctanoate production workers, with serum PFOA concentrations of 114,100 ng/mL [10].

Studies in rats and monkeys suggest that PFOA is correlated with multiple toxicities, including hepatotoxicity, carcinogenicity, immunotoxicity and developmental effects [6,11–13]. The liver has been demonstrated to be a primary bioaccumulative and target organ in rodent toxicity studies [14]. Liver toxicities such as liver enlargement, liver tumor, hepatocellular hypertrophy and vacuolation and lipid metabolism disorder are reportedly initiated by the activation of peroxisome proliferator-activated receptors (PPARs) [11,15]. Additionally, some rodent studies using knockout mice suggest that PPARs may not be the only pathways activated by PFOA [16–18]. Recently, human cell line *in vitro* studies showed that PFOA

* Corresponding author.
E-mail address: daijy@ioz.ac.cn (J. Dai).
[1] Hongxia Zhang and Ruina Cui contributed equally to this paper.

http://dx.doi.org/10.1016/j.jhazmat.2016.03.077
0304-3894/

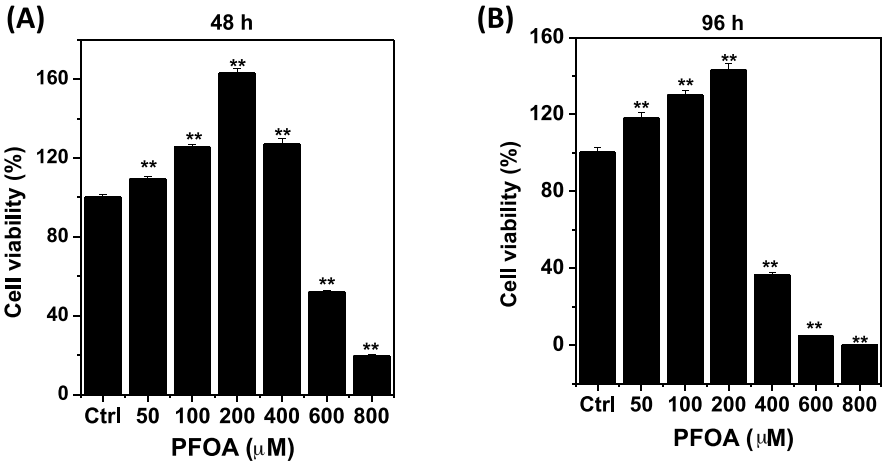

Fig. 1. Cell viability of HL-7702 cells exposed to PFOA for 48 h (A) and 96 h (B). Data are presented as means ± SE of three independent experiments. $^{*}p < 0.05$, $^{**}p < 0.01$.

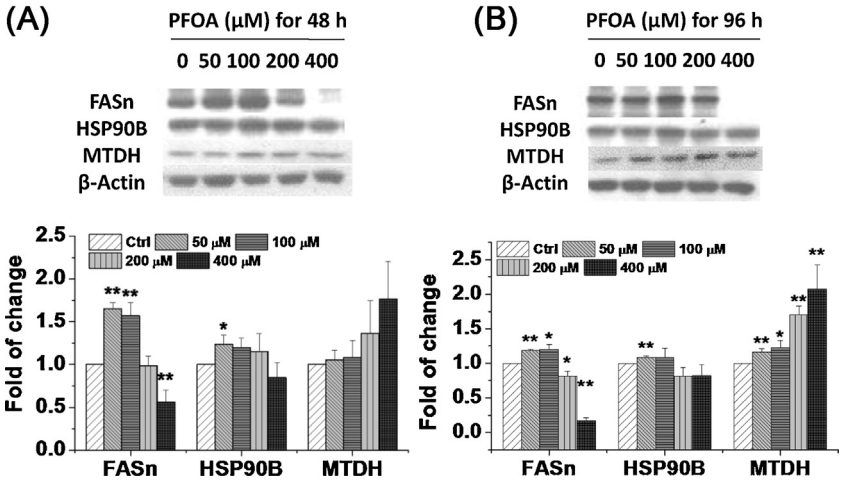

Fig. 2. Western blot verification of proteins identified in the iTRAQ results following PFOA exposure for 48 h (A) and 96 h (B). Left panel shows representative blots from three experiments. Right panel shows mean levels of protein bands compared with the control. Data are means ± SE ($n = 3$). $^{*}p < 0.05$, $^{**}p < 0.01$ compared with control.

can induce reactive oxygen species [19], inhibit HNF4α expression [20], perturb the cell cycle and induce apoptosis and DNA breaks in HepG2 cells [19,21]. An induction of glutathione- S-transferase Pi (GSTP) aberrant methylation by PFOA was also observed in human L02 cells [22]. Moreover, epidemiological and medical surveillance studies have reported inconsistent associations between PFOA and liver enzymes. Transaminase (ALT) levels, a marker of hepatocellular damage, were found to be positively associated with PFOA concentrations in some occupational and general population studies [23,24], but not in others [25].

Additionally, PFOA has a longer elimination half-life in humans (about 3.8 years) than that in rodents (4–19 days) [6], and thus might have higher accumulation. In humans, however, the causal biochemical mechanisms of hepatic toxicity after PFAA exposure are not clearly defined. PPARα-related responses in human liver cells are quantitatively and qualitatively different than those observed in rodents, therefore rodent data may not be a relevant indicator of PFAA risk in humans [26]. Thus, human hepatotoxicity to PFOA and its mechanism of action needs further research.

Proteomic technologies have been successfully used in toxicology studies. Isobaric tags for relative and absolute quantitation (iTRAQ) is one of the most widely used approaches. Using iTRAQ combined with 2D liquid chromatography and tandem mass spectrometry (2DLC–MS/MS), we identified the differentially expressed proteins in a human non-tumor liver cell line (HL-7702) after PFOA exposure. Through bioinformatic analysis, we found over one hundred proteins were related to cell proliferation and apoptosis. Therefore, we further detected the cell cycle by flow cytometer analysis and analyzed the protein levels of its regulators by western blot to confirm the effect and explore the mechanisms of PFOA on human liver cells.

2. Materials and methods

2.1. Cell culture, treatment and cell viability assay

HL-7702 cells are immortalized non-tumor cells derived from primary normal human hepatocytes, expressing a distinct ultrastructure compared to hepatic carcinoma cells and are considered as an ideal *in vitro* model of a Chinese nonmalignant liver [27]. The HL-7702 cells were obtained from the Shanghai Institute of Cell Biology, Chinese Academy of Sciences. The cells were cultured in RPMI-1640 complete culture medium containing 2.05 mM L-glutamine, 10% heat-inactivated fetal bovine serum, 100 IU/mL penicillin and 100 g/mL streptomycin at 5% CO_2 and 37 °C.

For cell viability assay, cells were seeded on 96-well plates at a density of 1×10^4 cells/well and 3×10^3 cells/well for 48 h and 96 h exposure, respectively. After 24 h cultured, the cells were treated

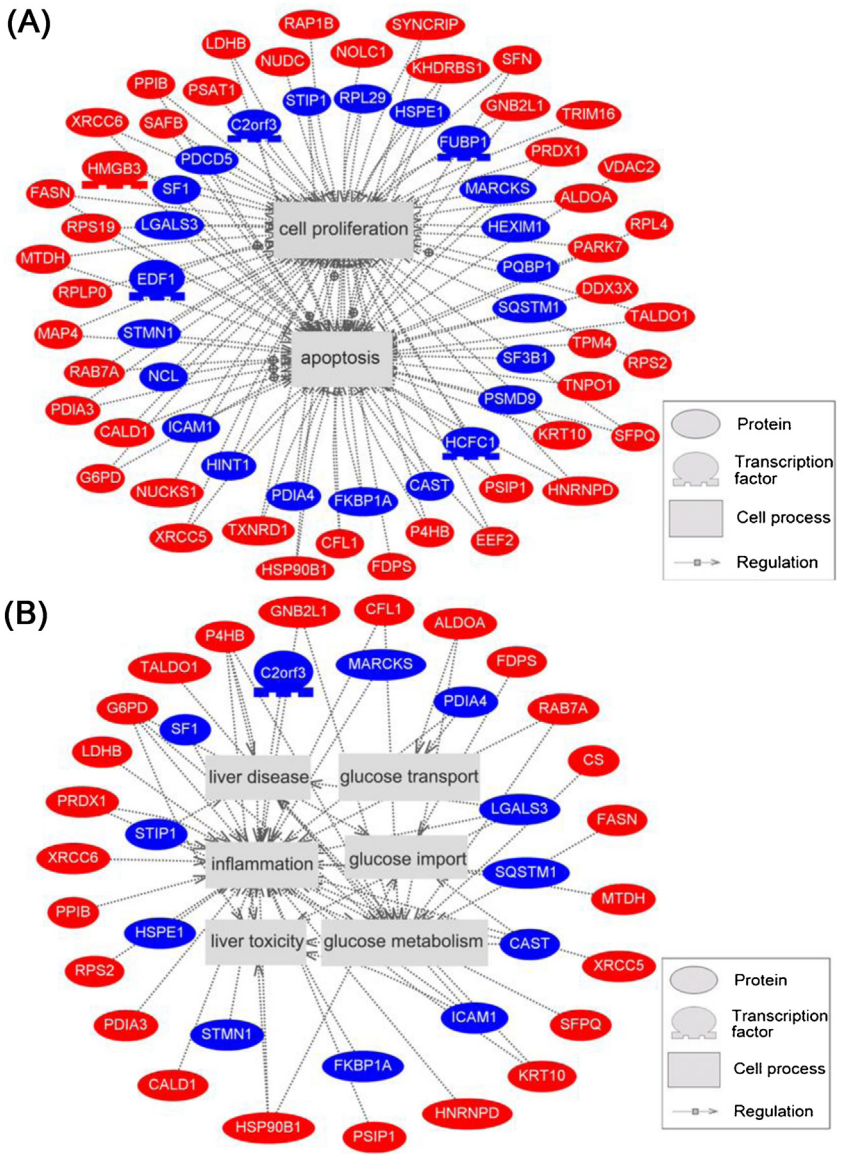

Fig. 3. Pathway studio analysis of differentially expressed proteins in human HL-7702 cells exposed to 50 μM PFOA for 48 h and 96 h. (A) A total of 68 proteins were related to cell proliferation and apoptosis. (B) Network of proteins related to liver disease and metabolism. Red bottom represents the upregulated proteins in response to 50 μM PFOA exposure. Blue bottom represents the downregulated proteins in 50 μM PFOA exposure. Full names of proteins are referred to in Table 1. (For interpretation of the references to color in this figure legend, the reader is referred to the web version of this article).

with PFOA in a range of concentrations (0–800 μM dissolved in 0.1% DMSO), and were cultured for 48 h and 96 h, separately. Cellular viability was determined using the MTT method. Absorbance at 490 nm was read using a Synergy microplate reader (BioTek, USA). The relative cellular viability (%) was calculated as: cellular viability (%) = $(OD_{treated}/OD_{control}) \times 100\%$.

2.2. Protein preparation, iTRAQ labeling and 2D LC–MS/MS

For iTRAQ analysis, HL-7702 cells were seeded onto 6-well culturing plates at an appropriate density and cultured for 24 h before treatment. After treatment with 50 μM of PFOA for 48 h and 96 h (PFOA/48 h and PFOA/96 h), the cells in three wells with the same treatment were collected and pooled into one sample. This experiment was repeated on two separate occasions. Two biological replicates in both the control (Ctrl) and PFOA-treated groups were prepared and analyzed by iTRAQ-based LC-ESI MS/MS according to the previous descriptions [28]. The tryptic peptides were labelled according to the kit protocol (ABI, Foster City, USA) with isobaric tags as follows: Tag113, PFOA-48 h; Tag 115, Ctrl-48 h; Tag 117, PFOA-96 h; and Tag 119, Ctrl-96 h (Fig. S1).

2.3. Protein identification and quantification

The resulting MS/MS spectra were combined and searched against the International Protein Index (IPI) human sequence database (version v3.76, HUMAN, 89378 sequences) with MASCOT software (Matrix Science, London, UK; version 2.3.02). For spectra search and protein identification, the search parameters were as previously reported [28]. Only the unique peptides were used to quantify the protein. According to the relative quantification and statistical analysis provided by Mascot software, we selected significantly overexpressed proteins using the following criteria: (1) the proteins were detected in both replicates; (2) the relative quantification *p*-value were below 0.05 in each replicate; and (3) the proteins were upregulated in both replicates or downregulated in both replicates.

To gain an overview of these data in relation to published literature, Pathway Studio software (version 6.5, Ingenuity Systems, Inc., Redwood City, CA, USA) was used.

2.4. Cell number measurement, flow cytometer analysis of cell cycle and western blot analysis

The HL-7702 cells were seeded in 6-well plates at an initial density of 2×10^5 cells/well and 8×10^4 cells/well, and then exposed to increasing concentrations of PFOA (0–400 μM in 0.1% DMSO) for 48 h and 96 h exposure, respectively. For cell number measurement, cells were harvested, washed and suspended in an equal volume of phosphate-buffered saline (PBS, pH 7.4). Cell number was calculated by a Bio-Rad TC10 automated cell counter using 10 μL of cell suspension. For cell cycle and western blot analysis, the details are given in Supplementary material.

2.5. Statistical analyses

For cell viability, cell number, cell cycle and western blot analysis, the data were presented as the means ± standard error (SE) for each experimental group of at least three individual samples. Differences between the control and treatment groups were analyzed by one-way ANOVA followed by Duncan's multiple range tests using SPSS 17.0. Probabilities of $p < 0.05$ were considered statistically significant.

3. Results

3.1. Cytotoxicity of PFOA

MTT analysis was used to analyze the cytotoxicity of PFOA to HL-7702 cells. As shown in Fig. 1, exposure to lower doses of PFOA (50, 100 and 200 μM) significantly increased cell viabilities in a dose-dependent manner after 48 h and 96 h. However, cell viabilities showed dose-dependent decreases when the doses of PFOA were above 400 μM. Cell viabilities were inhibited significantly at 400 μM PFOA treatment for 96 h and at 600 μM PFOA treatment for 48 h, and the inhibition rates were up to 30% and 60% of the control, respectively.

3.2. iTRAQ analysis and reproducibility

To understand global proteomic alteration in the HL-7702 cells after 50 μM PFOA treatment for 48 h and 96 h, iTRAQ analysis with isobaric tag labeling coupled with LC–MS/MS analysis were used. The entire experiment was replicated from cell treatment to LC–MS/MS analysis (Bio1 and Bio2). A total of 6571 and 6656 unique peptides from 2025 and 2048 proteins were identified in the two replicates, respectively (Supplemental Table S1), with 1670 proteins (69.5%) out of 2403 (total) proteins shared in both replicates. In addition, 82.5% of proteins detected in Bio1 were also identified in Bio2, and 81.5% proteins in Bio2 were also identified in Bio1, showing a high correction rate between the two replicates. In our iTRAQ data, the coverage levels of both biological replicates were 88.8% and 92.3% when the cutoff point was at ±50% variation for 48 h and 96 h, respectively (Supplemental Table S2), indicating good repeatability among the biological replicates of each group.

3.3. Differentially expressed proteins in HL-7702 cells after PFOA exposure

Because iTRAQ quantification underestimates 'real' fold change between samples [29], the proteins both upregulated or both downregulated significantly in the two replicates were chosen for further analysis. A total of 111 proteins were significantly differentially expressed after 50 μM PFOA treatment, including 86 proteins in the PFOA-48 h group and 29 proteins in the PFOA-96 h group compared with that in the control (Table 1). For most proteins (95.5%), the average iTRAQ ratios of the two replicates were above 1.2 or below 0.83. Additionally, we randomly chose three proteins, that is, fatty acid synthase (FASn), endoplasmin (HSP90B)

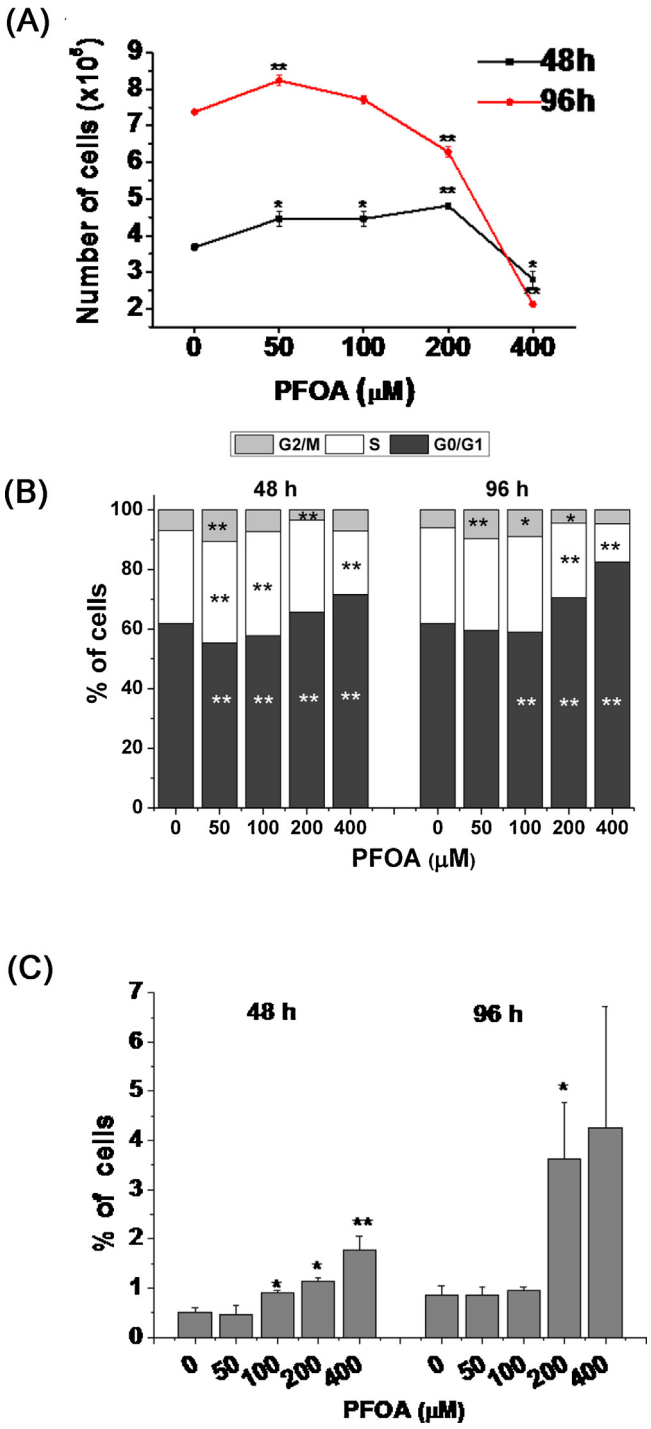

Fig. 4. Effect of PFOA on cell number and cell cycle status in HL-7702 cells. (A) Cell numbers of PFOA-exposed HL-7702 cells after 48 h and 96 h, counted by a cell counter. (B) Flow cytometric analysis of cell cycle distribution of HL-7702 cells. DNA distribution histogram of HL-7702 cells is shown. (C) Cell apoptotic rates (sub-G1 cell fragments) of HL-7702 cells exposed to PFOA by flow cytometry analysis. Values are means ± SE ($n = 3$). * $p < 0.05$, ** $p < 0.01$ compared with control.

Table 1
Differentially expressed proteins identified by iTRAQ analysis in human HL-7702 cells in response to PFOA exposure.

			48 h Ratio (113:115)		96 h Ratio (119:117)		
Accession	Gene symbol	Full name	Bio1	Bio2	Bio1	Bio2	Biological function
Upregulated							
IPI00030706	AHSA1	Activator of 90 kDa heat shock protein ATPase homolog 1	**1.86***	**1.76***	1.39	0.89	Protein folding
IPI00465439	ALDOA	Fructose-bisphosphate aldolase A	**1.69***	**1.50***	1.04	1.08	Glycolysis/gluconeogenesis, cytoskeleton
IPI00215918	ARF4	ADP-ribosylation factor 4	**2.90***	**2.09***	1.15	1.07	Signal transduction
IPI00006079	BCLAF1	Isoform 1 of Bcl-2-associated transcription factor 1	0.93	0.97	**2.03***	**1.52***	Apoptosis, gene expression
IPI00218694	CALD1	Isoform 2 of Caldesmon	0.77	0.60	**1.35***	**1.29***	Muscle system process, cell motion, cytoskeleton
IPI00302925	CCT8	59 kDa protein, chaperonin containing TCP1, subunit 8 (theta)	**1.55***	**1.67***	0.96	0.88	Protein folding
IPI00012011	CFL1	Cofilin-1	**1.31***	**1.62***	1.06	1.05	Cell migration, cytoskeleton, cell death
IPI00020510	CISD1	CDGSH iron-sulfur domain-containing protein 1	0.60	0.50	**1.36***	**1.50***	Cellular respiration
IPI00025366	CS	Citrate synthase, mitochondrial	**1.67***	**1.5***	0.64*	0.72	TCA cycle, glyoxylate and dicarboxylate metabolism
IPI00215637	DDX3X	ATP-dependent RNA helicase DDX3X	**1.33***	**1.54***	1.12	0.93	Signal transduction, ribosome biogenesis
IPI00186290	EEF2	Elongation factor 2	**1.22***	**1.52***	0.96	0.93	Translation
IPI00220797	ENSA	Isoform 2 of Alpha-endosulfine	1.11	1.02	**1.82***	**1.84***	Response to nutrient, cell cycle, mitosis
IPI00026781	FASN	Fatty acid synthase	**1.17***	**1.26***	0.81*	1.08	Lipid metabolism
IPI00914566	FDPS	Farnesyl pyrophosphate synthase	**1.35***	**1.88***	0.88	0.93	Sterol metabolism, lipid metabolism
IPI00216008	G6PD	Isoform Long of Glucose-6-phosphate 1-dehydrogenase	**1.32***	**1.58***	0.85	0.80*	Glucose/steroid/lipid metabolic process
IPI00004669	GALNT2	Polypeptide *N*-acetylgalactosaminyl transferase 2	**1.35***	**1.94***	0.80*	0.88	Immune effector process, glycan biosynthesis
IPI00848226	GNB2L1	Guanine nucleotide-binding protein subunit beta-2-like 1	**1.48***	**1.66***	0.93	0.74	Apoptosis, cell cycle, translation regulation
IPI00026272	HIST1H2AE	Histone H2A type 1-B/E	**1.20***	**1.20***	1.08	1.07	Nucleosome organization
IPI00018534	HIST1H2BL	Histone H2B type 1-L	**1.27***	**1.34***	0.70*	0.75	Nucleosome organization
IPI00217477	HMGB3	High mobility group protein B3	1.15	1.21	**1.32***	**1.35***	Immune response
IPI00028888	HNRNPD	Isoform 1 of Heterogeneous nuclear ribonucleoprotein D0	**1.32***	**1.24***	1.15	1.10	RNA splicing
IPI00012074	HNRNPR	Isoform 1 of Heterogeneous nuclear ribonucleoprotein R	**1.28***	**1.26***	1.02	1.04	RNA splicing
IPI00027230	HSP90B1	Endoplasmin	**1.38***	**1.45***	1.08	1.01	Protein folding, cell death, apoptosis
IPI00008575	KHDRBS1	Isoform 1 of KH domain-containing, RNA-binding, signal transduction-associated protein 1	1.18	1.06	**1.27***	**1.40***	Cell cycle, cell proliferation, transcription
IPI00009865	KRT10	Keratin, type I cytoskeletal 10	**3.73***	**5.25***	0.78	0.82	Cytoskeleton
IPI00219217	LDHB	L-lactate dehydrogenase B chain	**1.55***	**1.42***	1.02	0.94	Glycolysis/gluconeogenesis, pyruvate metabolism
IPI00880007	MAP4	Microtubule-associated protein	0.63*	0.63	**1.14***	**1.14***	No annotation
IPI00328715	MTDH	Protein LYRIC	0.91	0.72*	**1.30***	**1.29***	Gene expression
IPI00216654	NOLC1	Isoform Beta of Nucleolar and coiled-body phosphoprotein 1	0.87	0.86	**1.40***	**1.33***	RNA processing, cell cycle, ribosome biogenesis
IPI00294891	NOP2	Isoform 1 of Putative ribosomal RNA methyltransferase NOP2	0.70	0.55*	**1.46***	**1.18***	RNA processing, ribosome biogenesis
IPI00022145	NUCKS1	Isoform 1 of Nuclear ubiquitous casein and cyclin-dependent kinases substrate	1.03	1.23	**1.53***	**1.53***	No annotation
IPI00550746	NUDC	Nuclear migration protein nudC	**1.31***	**1.33***	1.07	1.02	Cell cycle, cell proliferation, response to hormone stimulus
IPI00010796	P4HB	Protein disulfide-isomerase	**1.24***	**1.19***	1.09	1.06	Cell redox homeostasis
IPI00298547	PARK7	Protein DJ-1	**1.26***	**1.22***	1.05	0.94	Cell death, stress response, inflammatory response
IPI00025252	PDIA3	Protein disulfide-isomerase A3	**1.34***	**1.28***	0.87	1.02	Cell death, cell redox homeostasis
IPI00646304	PPIB	Peptidyl-prolyl *cis*-trans isomerase B	**1.67***	**1.77***	1.11	1.06	Protein folding
IPI00000874	PRDX1	Peroxiredoxin-1	**1.36***	**1.6***	0.93	0.88	Response to oxidative stress
IPI00001734	PSAT1	Phosphoserine aminotransferase	**1.25***	**1.48***	1.04	1.23	Glycine, serine and threonine metabolism
IPI00028122	PSIP1	Isoform 1 of PC4 and SFRS1-interacting protein	1.00	1.08	**1.49***	**1.39***	DNA metabolic process, transcription regulation
IPI00291922	PSMA5	Proteasome subunit alpha type-5	**1.73***	**1.95***	0.73*	0.87	Cell cycle, apoptosis, gene expression
IPI00016342	RAB7A	Ras-related protein Rab-7a	**1.32***	**1.46***	1.05	0.93	Signal transduction, protein transport
IPI00015148	RAP1B	Ras-related protein Rap-1b	**1.94***	**1.62***	0.96	1.03	Signal transduction, cell proliferation,

Table 1 (*Continued*)

Accession	Gene symbol	Full name	48 h Ratio (113:115)		96 h Ratio (119:117)		Biological function
			Bio1	Bio2	Bio1	Bio2	
IPI00182533	RPL28	60S ribosomal protein L28	**1.81***	**1.82***	1.45	1.08	Translation, ribosome structure
IPI00003918	RPL4	60S ribosomal protein L4	**1.98***	**1.53***	1.12	1.08	Ribosome structure
IPI00008530	RPLP0	60S acidic ribosomal protein P0	**1.55***	**1.43***	1.12	1.12	Translation, ribosome structure
IPI00215780	RPS19	40S ribosomal protein S19	**1.29***	**1.41***	1.26*	1.17	Translation, ribosome structure
IPI00013485	RPS2	40S ribosomal protein S2	**1.42***	**1.45***	1.00	1.00	Translation, ribosome structure
IPI00300631	SAFB	Scaffold attachment factor B1	0.89	1.00	**1.21***	**1.26***	Transcription
IPI00013890	SFN	Isoform 1 of 14-3-3 protein sigma	**1.36***	**1.47***	1.11	1.06	Cell growth, cell cycle, apoptosis
IPI00010740	SFPQ	Isoform Long of Splicing factor, proline- and glutamine-rich	**1.36***	**1.36***	1.09	1.13*	Stress response, nucleotide metabolic process
IPI00018140	SYNCRIP	Isoform 1 of Heterogeneous nuclear ribonucleoprotein Q	**1.39***	**1.59***	1.01	1.11	RNA processing
IPI00744692	TALDO1	Transaldolase	**1.61***	**1.33***	0.87	0.97	Glucose metabolic process
IPI00024364	TNPO1	Isoform 1 of Transportin-1	**1.57***	**1.42***	1.00	1.04	Signal sequence binding, protein assembly
IPI00220709	TPM2	Isoform 2 of Tropomyosin beta chain	1.09	1.18	**1.71***	**1.40***	Cytoskeleton
IPI00010779	TPM4	Isoform 1 of Tropomyosin alpha-4 chain	0.83	0.85*	**1.26***	**1.32***	Cell motion, cardiac muscle contraction
IPI00007955	TRIM16	Isoform 1 of Tripartite motif-containing protein 16	1.43	1.27	**3.06***	**2.52***	Zinc ion binding
IPI00554786	TXNRD1	Isoform 5 of Thioredoxin reductase 1, cytoplasmic	**1.19***	**1.40***	1.07	0.89*	Cell proliferation, cell redox homeostasis
IPI00024145	VDAC2	Isoform 2 of Voltage-dependent anion-selective channel protein 2	**1.61***	**1.62***	0.90	0.94	Ion transport, calcium signaling pathway
IPI00220834	XRCC5	X-ray repair cross-complementing protein 5	**1.53***	**1.56***	1.02	0.93	DNA repair, apoptosis, cell death
IPI00644712	XRCC6	X-ray repair cross-complementing protein 6	**1.29***	**1.33***	1.05	1.00	DNA repair, apoptosis, cell death
IPI00029400	ZRANB2	Isoform 1 of Zinc finger Ran-binding domain-containing protein 2	0.83	0.96	**1.40***	**1.27***	RNA splicing
Downregulated							
IPI00299024	BASP1	Isoform 1 of Brain acid soluble protein 1	**0.51***	**0.51***	1.22	1.17	No annotation
IPI00217121	C19orf21	Uncharacterized protein C19orf21	**0.45***	**0.43***	0.98	0.68	No annotation
IPI00418340	C2orf3	Isoform 1 of GC-rich sequence DNA-binding factor	**0.41***	**0.58***	1.12	1.10	Transcription
IPI00220857	CAST	Isoform 2 of Calpastatin	**0.50***	**0.71***	1.03	1.32	Syncytium formation, muscle cell differentiation
IPI00015894	CDC42EP4	Cdc42 effector protein 4	**0.43***	**0.56***	1.08	0.91	Signal transduction
IPI00217541	DDX51	ATP-dependent RNA helicase DDX51	**0.55***	**0.50***	1.26	1.16	Ribosome biogenesis
IPI00465045	DIP2B	Disco-interacting protein 2 homolog B	**0.50***	**0.56***	0.81	0.80	Transcription factor binding
IPI00006362	EDF1	Isoform 2 of Endothelial differentiation-related factor 1	**0.58***	**0.46***	1.15*	1.45	Transcription, lipid metabolism, cell differentiation
IPI00759644	FKBP1A	Peptidyl-prolyl *cis*-trans isomerase FKBP1A isoform b	**0.59***	**0.52***	0.88	0.81	No annotation
IPI00060521	FLYWCH2	FLYWCH family member 2	**0.36***	**0.40***	1.15	1.16*	No annotation
IPI00375441	FUBP1	Isoform 1 of Far upstream element-binding protein 1	**0.59***	**0.60***	1.19*	1.12	Transcription
IPI00019848	HCFC1	Isoform 1 of Host cell factor 1	**0.57***	**0.51***	0.94	1.01	Transcription, cell cycle
IPI00007941	HEXIM1	Hexamethylene bis-acetamide inducible 1	**0.64***	**0.58***	1.00	1.17	Transcription
IPI00239077	HINT1	Histidine triad nucleotide-binding protein 1	**0.83***	**0.87***	0.93	0.84*	Tumor suppressor
IPI00000335	HINT2	Histidine triad nucleotide-binding protein 2, mitochondrial	0.76	0.74	**0.80***	**0.76***	Apoptosis, steroid biosynthetic process
IPI00220362	HSPE1	10 kDa heat shock protein, mitochondrial	**0.78***	**0.79***	1.08	1.12*	Apoptosis, response to organic substance
IPI00008494	ICAM1	Intercellular adhesion molecule 1	**0.67***	**0.72***	0.94	0.87	Adaptive immune response
IPI00465431	LGALS3	Galectin-3	**0.66***	**0.54***	0.76*	0.98	Skeletal system development
IPI00291328	NDUFV2	NADH dehydrogenase [ubiquinone] flavoprotein 2, mitochondrial	**0.73***	**0.76***	**0.78***	**0.70***	Electron transport
IPI00002525	NENF	Neudesin	**0.74***	**0.74***	1.07	1.08	Signal transduction
IPI00337541	NNT	NAD(P) transhydrogenase, mitochondrial	0.91	0.96	**0.81***	**0.80***	TCA cycle, ion transport, cellular respiration
IPI00002349	NUFIP2	Nuclear fragile X mental retardation-interacting protein 2	**0.55***	**0.63***	1.05	0.93	RNA binding
IPI00329650	NUP35	Nucleoporin NUP53	0.95	0.62*	**0.63***	**0.67***	RNA/protein localization, transport
IPI00023640	PDCD5	Programmed cell death protein 5	**0.44***	**0.70***	0.86	0.97	Apoptosis, cell death
IPI00009904	PDIA4	Protein disulfide-isomerase A4	1.09	1.15	**0.85***	**0.87***	Cell redox homeostasis
IPI00386483	PQBP1	Isoform 4 of polyglutamine-binding protein 1	**0.68***	**0.55***	1.07	0.90	Transcription
IPI00026154	PRKCSH	cDNA FLJ59211, highly similar to Glucosidase 2 subunit beta	**0.84***	**0.79***	1.05	1.12	Signal transduction
IPI00010860	PSMD9	Isoform p27-L of 26S proteasome non-ATPase regulatory subunit 9	**0.61***	**0.61***	0.93	0.97	Cell cycle, proteasomal protein catabolic process
IPI00020436	RAB11B	Ras-related protein Rab-11B	1.18	1.04	**0.84***	**0.74***	Signal transduction, protein transport
IPI00013174	RBM14	Isoform 1 of RNA-binding protein 14	**0.58***	**0.45***	0.96	0.98	Transcription
IPI00419919	RPL29	Ribosomal protein L29	**0.75***	**0.64***	1.07	1.05	Translation, ribosome structure

Table 1 (*Continued*)

Accession	Gene symbol	Full name	48 h Ratio (113:115)		96 h Ratio (119:117)		Biological function
			Bio1	Bio2	Bio1	Bio2	
IPI00037619	RPL39P5	Putative 60S ribosomal protein L39-like 5	**0.32***	**0.40***	0.49	0.79	Translation, ribosome structure
IPI00008527	RPLP1	60S acidic ribosomal protein P1	**0.54***	**0.62***	1.08	0.79*	Translation, ribosome structure
IPI00008438	RPS10	40S ribosomal protein S10	0.90	0.94	**0.80***	**0.73***	Translation, ribosome structure
IPI00013917	RPS12	40S ribosomal protein S12	0.73	0.97	**0.72***	**0.76***	Translation, ribosome structure
IPI00641384	SEC16A	Protein transport protein Sec16A	**0.49***	**0.53***	0.89	1.09	Blood vessel development
IPI00294627	SF1	Isoform 2 of Splicing factor 1	**0.75***	**0.67***	1.14	0.95	RNA splicing, cell cycle, signal transduction
IPI00026089	SF3B1	Splicing factor 3B subunit 1	**0.70***	**0.74***	1.18	1.10	RNA processing
IPI00006863	SPAG7	Sperm-associated antigen 7	**0.71***	**0.61***	1.11	1.09	Nucleic acid binding
IPI00179473	SQSTM1	Isoform 1 of Sequestosome-1	**0.67***	**0.61***	0.95	0.81	Apoptosis, cell death, immune response, gene expression
IPI00215884	SRSF1	Isoform ASF-1 of Serine/arginine-rich splicing factor 1	**0.84***	**0.81***	0.89*	0.96	RNA processing
IPI00010204	SRSF3	Serine/arginine-rich splicing factor 3	**0.51***	**0.51***	**0.68***	**0.63***	RNA processing
IPI00013894	STIP1	Stress-induced-phosphoprotein 1	**0.73***	**0.84***	1.10*	1.07	Stress response
IPI00479997	STMN1	Isoform 1 of Stathmin	**0.58***	**0.62***	1.17	1.33*	MAPK signaling pathway
IPI00328840	THOC4	THO complex subunit 4	**0.67***	**0.67***	1.06	1.23	RNA splicing, transport
IPI00104050	THRAP3	Thyroid hormone receptor-associated protein 3	**0.56***	**0.63***	1.17	1.24*	Transcription, signal transduction
IPI00027107	TUFM	Elongation factor Tu, mitochondrial precursor	1.22*	0.99	**0.83***	**0.84***	Translation
IPI00444371	WDR44	Isoform 1 of WD repeat-containing protein 44	**0.71***	**0.76***	1.13	1.10	Cell migration
Down-up regulated							
IPI00219301	MARCKS	Myristoylated alanine-rich C-kinase substrate	**0.67***	**0.51***	**1.39***	**1.45***	Energy metabolic process, signal transduction
IPI00604620	NCL	Nucleolin	**0.86***	**0.85***	**1.11***	**1.21***	Blood vessel development

The 111 unique proteins were detected in both biological replicates (Bio1 and Bio2). Protein ratio was calculated from at least two unique peptides. *$p < 0.05$. Proteins that changed significantly in both replicates ($p < 0.05$, ratios in bold) were clustered based on similar trends after PFOA exposure.

and metadherin (MTDH), to validate the iTRAQ results by western blot analysis (Fig. 2). The protein levels of FASn, HSP90B and MTDH showed similar change trends with the iTRAQ analysis, although the responses of FASn and HSP90B were significant at 96 h. This suggests that the filter criteria used for choosing differentially expressed proteins was suitable in this study.

3.4. Bioinformatics analysis for differentially expressed proteins

Using Pathway Studio analysis, most proteins were found to be associated with cell proliferation and apoptosis, and included 45 upregulated and 23 downregulated proteins. Thereinto, 46 of these proteins were related to both cell proliferation and apoptosis, including FASn, MTDH, 14-3-3 protein sigma (SFN), calpastatin (CAST) and protein disulfide-isomerase (PDIA3) (Fig. 3A). In addition, 36 proteins were associated with hepatic injury and disease and glucose metabolism (Fig. 3B), which were all present in Fig. 3A except citrate synthase (CS). Thereinto, 29 of these proteins (including 18 upregulated and 11 downregulated proteins) were related to inflammation such as peroxiredoxin-1 (PRDX1), PDIA3, stathmin (STMN1) and so on. Additionally, 14 proteins were related to glucose metabolism and transport, twelve of which were upregulated, including FASn, transaldolase (TALDO1), fructose-bisphosphate aldolase A (ALDOA) and isoform long of glucose-6-phosphate 1-dehydrogenase (G6PD).

3.5. Cell proliferation in HL-7702 cells exposed to PFOA

Cell number was determined at different doses of PFOA, as shown in Fig. 4A. Except for the 400 μM PFOA group, HL-7702 cells showed a significant increase in cell number compared with that of the control at 48 h. However, at 96 h, cell number was increased significantly in the 50 μM PFOA group and inhibited significantly in the 200 μM and 400 μM PFOA groups. The cell numbers in the 400 μM PFOA group at 48 h and 96 h decreased to 0.76-fold and 0.29-fold that in the control group, respectively.

Cell proliferation depends on a continuous cell cycle. As shown in Fig. 4B, the proportions of HL-7702 cells in the G0/G1 phase decreased significantly from 61.8% to 55.4% and 57.8% after 50 and 100 μM PFOA exposure for 48 h, respectively. Meanwhile, the cells in the S phase significantly increased from 31.3% to 34.0% and 34.9% accompanied by an increase in G2/M phase cells from 6.9% to 10.6% and 7.3% after 50 and 100 μM PFOA exposure for 48 h, respectively. In contrast, after 200 and 400 μM PFOA exposure for 48 h, cells in the G0/G1 phase increased significantly compared with that in the control, corresponding to an obvious decrease in cells in both the S and G2/M phases. The same change trends were observed in HL-7702 cells exposed to different doses of PFOA at 96 h. These results show that PFOA doses of 50 and 100 μM promoted HL-7702 cells from the G1 phase to the S phase, whereas 200 and 400 μM PFOA blocked cells in the G0/G1 phase. Additionally, although the percentages of sub-G1 cell fragments increased after 100–400 μM PFOA treatment for 48 h and 200 μM PFOA treatment for 96 h compared with the control, the ratios were all less than 5% (Fig. 4C), suggesting there were no significant differences in apoptosis ratios between the control and PFOA-treated groups. These data indicate that although there were significant decreases in cell number and cell viability after 200 and 400 μM PFOA exposure, few cells underwent apoptosis.

3.6. PFOA-altered expression of regulatory proteins involved in cell cycle and apoptotic cell death

To further verify the effect of PFOA on the HL-7702 cell cycle, cell cycle signaling molecules were evaluated, including positive cell cycle-regulators (cyclins and cyclin-dependent kinases (CDKs)) and negative regulators (p53, p21, MYT1 and WEE1). Cyclin D1/CDK6, cyclin E/CDK2, cyclin A2/CDK2 and cyclin B1/CDK complexes play important roles in controlling G1 progression, G1/S transition and G2 and M progression. As shown in Fig. 5A, low doses of PFOA (50 or 100 μM) significantly enhanced the expression levels of cyclin D1, CDK6, cyclin E2, cyclin A2, CDK2, *p*-CDK1(Y15), p53, p21,

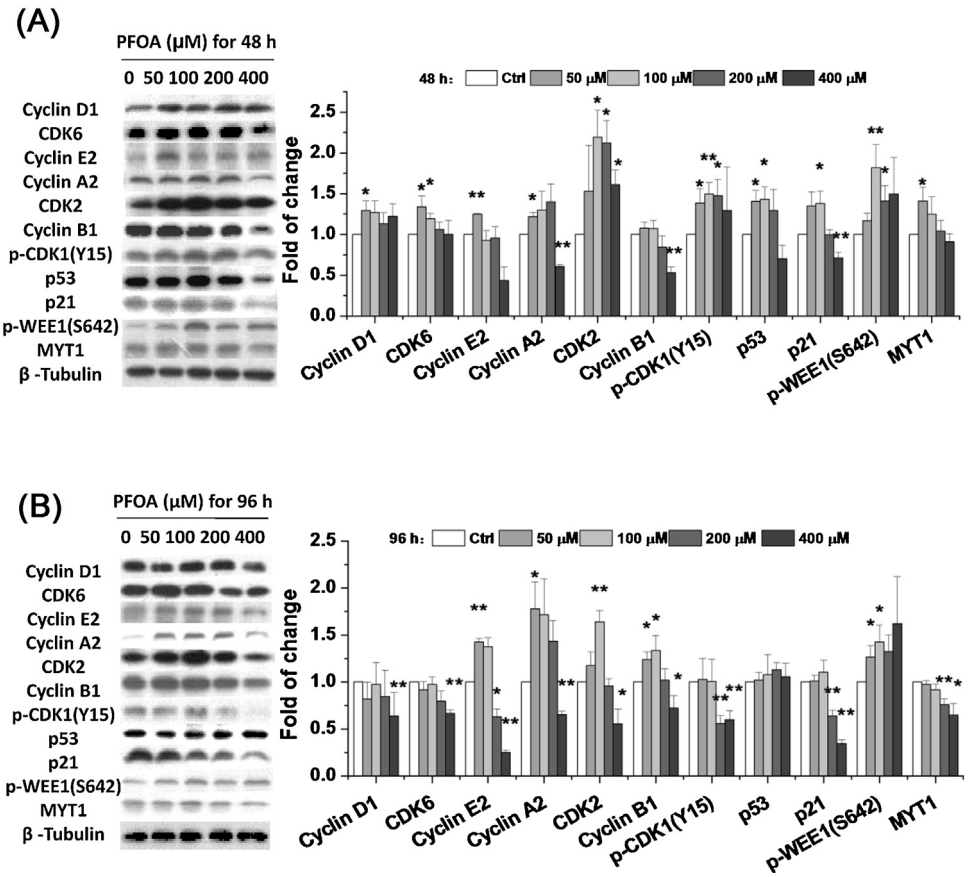

Fig. 5. Protein levels of cell cycle-related proteins in HL-7702 cells after PFOA exposure for 48 h (A) and 96 h (B). Data of treatments were calibrated to the control values (control = 1). Data are means ± SE ($n = 3$) from three independent experiments in triplicate. * $p < 0.05$, ** $p < 0.01$ compared with control.

p-WEE1 (S642) and MYT1, while high doses of PFOA (400 μM) significantly inhibited the protein levels of cyclin A1, cyclin B1 and p21 at 48 h. The levels of CDK2 were also upregulated in both 200 and 400 μM PFOA groups, while that of *p*-CDK1 (Y15) and *p*-WEE1 (S642) were significantly induced only in the 200 μM PFOA group at 48 h. Additionally, after 96 h, PFOA markedly increased the protein expressions of cyclin E2, cyclinA2, CDK2, cyclin B1 and *p*-WEE1 (S642) at 50 and 100 μM PFOA, and then caused a marked decrease in the expression levels of almost all proteins detected, except for p53 and *p*-WEE1 (S642) at 200 and 400 μM (Fig. 5B).

3.7. Effect of PFOA on apoptosis-related proteins

To investigate the role of p53 in PFOA-induced changes in cell cycle progression, the expression levels of p53 relative apoptosis proteins were determined by western blot analysis, including pro-apoptotic protein (Bax) and anti-apoptotic proteins (Bcl-2 and Bcl-XL). As shown in Fig. 6A, the protein levels of Bcl-2 were significantly reduced after 400 μM PFOA treatment for 48 h, while Bcl-XL expression was significantly inhibited in the 100 and 400 μM PFOA groups. There were no obvious changes in the levels of Bax after PFOA exposure for 48 h. Following 96 h exposure, only the expression of Bcl-2 was significantly decreased in the 200 and 400 μM PFOA groups, with the other proteins showing no significant changes in levels after PFOA treatment, although there was an increasing trend in Bax with 100–400 μM PFOA exposure (Fig. 6B).

4. Discussion

In the present study, proteomic analysis was used to investigate the effect of PFOA on human liver hepatocytes. About half of the differentially expressed proteins were related to both cell proliferation and apoptosis. However, the changes in expression level of these proteins pointed to incompatible cellular processes. For example, decreased expression of STMN1 and CAST, which have been reported to prevent cell proliferation [30,31], implicated an enhanced apoptosis process in the HL-7702 cells after PFOA exposure. On the contrary, SFN is reported to protect cells against apoptosis [32]. In addition, the expression level of programmed cell death 5 (PDCD5) has been found to be reduced in several human tumors [33–37] and has been reported to markedly promote cell proliferation in Hela and HEK293 cell lines [38]. Thus, the increased expression of SFN and decreased expression of PDCD5 suggested an induction of cell proliferation and anti-apoptosis processes. To clarify whether PFOA promoted cell proliferation or apoptosis in human cells, we further analyzed the cell number and cell cycle status of the HL-7702 cells. Similar to the MTT assay results, HL-7702 cell numbers increased significantly upon exposure to low dosages of PFOA but showed decrease in higher dosage PFOA groups. Additionally, no effective apoptosis was observed even in 400 μM PFOA treated groups. However, the opposite effect has been observed in human hepatoma cell line (HepG2) and other non-tumor mammalian cell lines (Vero cells), with dose-dependent decreases in cell viability, and significant apoptosis was found in HepG2 and Vero cells after PFOA treatment at doses of 200 μM for 48 h and 500 μM for 24 h, respectively [21,39,40]. This suggests that HepG2

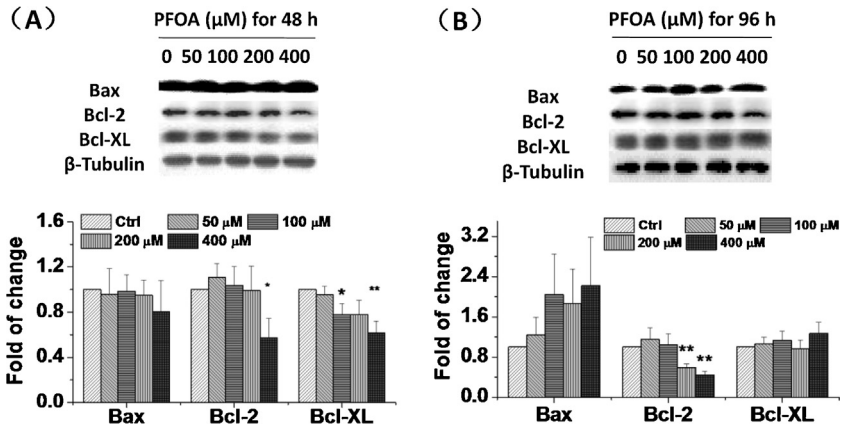

Fig. 6. Western blot analysis of p53-related apoptosis proteins in HL-7702 cells after PFOA exposure. Protein levels of Bax, Bcl-2 and Bcl-XL were detected in cells treated by PFOA for 48 h (A) and 96 h (B). Treatment data were calibrated to the control values (control = 1). Data are means ± SE ($n = 3$). Significantly different from control group ($^{*}p < 0.05$, $^{**}p < 0.01$).

and Vero cells might be more sensitive than HL-7702 cells to PFOA, which may be caused by the different genetic backgrounds of these cell lines. However, Huang et al. reported that 120 μM PFOA can induce apoptosis in the same HL-7702 cell line after 72 h exposure and identified several differentially expressed proteins related to cancer and cell death by proteomic study [41]. In addition, the change trends in several similar proteins, such as heterogeneous nuclear ribonucleoprotein C (HNRNPC), keratin 10 (KRT10) and protein disulfide isomerase (PDIA3), were opposite to that found in our 48 h-exposed HL-7702 cells. The low dose response in our study may be one of the reasons for the different proteomic results. Additionally, considering that the cell density before exposure in Huang's study was higher than that after PFOA treatment in our study, the different cell status and cell densities during exposure might also contribute to the different cell responses between the two studies.

Some cell cycle signaling molecules were determined to further explore the mechanism of the effect of PFOA on the cell cycle in HL-7702 cells. Cell cycle progression involves sequential activation of CDKs, which possess an association with corresponding regulatory cyclins necessary for their activation [42]. The cyclin D/CDK4/6 and cyclin E/CDK2 complexes regulate cell cycle transition from the G_1 to S phase [43]. Progression through the S phase requires cyclin A, which can also be assembled with CDK2 to form cyclin A/CDK2 complexes, providing a link between the early events in G1 and the final events that occur during the G2/M phase. In this study, the induction of cyclin D1, CDK6, cyclin E2, cyclin A2 and CDK2 in low-dose PFOA groups, associated with increased cell numbers in the S phase and loss of cells in the G0/G1 phase, indicated that cells were driven by PFOA into cell cycles from the G0 stage, with sequential acceleration in the transition of cells from the G1 to S phase. Once the S phase is complete, the cell enters the second growth phase (G2) where it prepares to begin mitosis. This entry into mitosis depends upon the activation of the cyclin B/CDK1 complex [44]. In the G2 phase, CDK1 is phosphorylated at Thr14 and Tyr15 by the protein kinases MYT1 and WEE1, thereby converting it into an inactive precursor [45]. The phosphorylation of WEE1 on Ser642 is reported to increase the stability of WEE1 in the nucleus by binding to 14-3-3β or σ [46]. Thus, the induced expressions of SFN, MYT1, *p*-WEE1 (S642) and *p*-CDK1 (Y15) at 48 h in our study suggested that low-dose PFOA had the potential to induce G2/M arrest, corresponding with an increased proportion of G2/M cells. We speculated that this might be a negative feedback response to the acceleration of cell cycle progression (especially G1/S phase transition), which aimed to retard cell proliferation by arrest in the G2/M phase, or could be attributed to DNA damage, which triggered the activation of the G2 checkpoint pathway. In the G2 checkpoint, p53, which is activated by CHK1 and ATM/ATR, transactivates p21 and upregulates the 14-3-3σ protein, which in turn inhibits the cyclin B/CDK1 complexes through phosphorylation of CDK1, thus keeping the cell arrested in G2 until the damage is fixed [47]. Therefore, the upregulation of p53 and p21 in the low-dose PFOA groups at 48 h implicated that DNA damage occurred in the HL-7702 cells. However, no changes in the expression levels of these proteins, except for *p*-WEE1 (S642), were observed in the low-dose PFOA groups at 96 h, corresponding with upregulation of cyclin B1 and no observation of G2/M arrest. However, whether DNA damage occurred still needs further study.

In contrast to 50 and 100 μM PFOA treatment, the decreased expression of most CDKs and cyclins in the 400 μM PFOA group showed obvious cell cycle arrest in the G0/G1 phase, concomitant with an increase in the proportion of cells in the G0/G1 phase and loss of cells in the (S + G2/M) phases. These results were consistent with early findings in other cell lines. Similarly, Huang et al. reported that PFOA arrested the HL-7702 cell cycle in the G2/M phase and induced cell apoptosis through the p53-dependent pathway [41]. In addition to G2/M arrest, induction of p21 in response to DNA damage can inhibit complex cyclin E/CDK2, leading to G1 arrest [43]. In this study, p53 expression did not change, but p21 was significantly downregulated after exposure to high doses of PFOA; thus, we speculated that G0/G1 arrest might be induced by the p53-independent pathway, for example, phosphorylation of phosphatase Cdc25A [43]. Additionally, the ratio of Bax to Bcl-2 is reportedly a critical determinant of a cell's threshold for undergoing apoptosis [48]. Therefore, 400 μM PFOA might be a threshold concentration to induce apoptosis in HL-7702 cells. Furthermore, the decrease in cell numbers in the high dose PFOA groups might be attributed to cell cycle arrest at the G0/G1 phase, and less to apoptosis. In addition, although limited in scope, available human data supported that PFOA was not expected to elicit a hepatocarcinogenic response in humans [49]. Thus, it is unknown whether cell proliferation was only a hormesis response induced by low doses of PFOA or related to hepatomegaly or hepatocarcinogenic potency of PFOA.

As a peroxisome proliferator, activation of PPARα is thought to be responsible for liver enlargement and hepatic tumor induction by PFOA in rodents through upregulation of specific subsets of genes involved in peroxisome proliferation and lipid metabolism, although potentially PPARα- independent effects were also observed in PFOA exposed rodent and non-rodent species [6,18,50,51]. We found that activation of PPARα-regulated transcription in HL-7702 cells was far less robust than that in

rodents (data not shown), consistent with the results in HepG2 cells [50]. Thus, cell proliferation observed in HL-7702 cells might be induced by PPARα-independent pathways. In addition, some differentially expressed proteins involved in lipid and glucose metabolic pathways were found in our proteomic results. Different from the response of rodents to PFOA, proteins associated with PPARα-dependent fatty acid oxidation were not changed in HL-7702 cells. Upregulation of farnesyl diphosphate synthetase (FDPS) might result in more production of squalene [52], the first specific intermediate in the cholesterol biosynthetic pathway while upregulation of FASN in HL-7702 cells may therefore increase long-chain fatty acid biosynthesis. This was consistent with reports of increased fatty acid synthesis, which might lead to hepatic steatosis, in PFOA exposed rodents [53]. Enhanced expression of genes associated with fatty acid and cholesterol synthesis were also observed in PFOA exposure mice in our previous study [54]. FDPS and FASN have been previously shown to be under transcriptional control of SREBP-1 [55,56], suggesting that SREBP-1 might represent an underlying mechanism in lipogenesis in HL-7702 cells induced by PFOA. Hence, our results supported the previous PFOA-induced hepatic steatosis findings in rodents. Human cells maintain their homeostasis through energy production via glucose catabolism. In the presence of oxygen, most differentiated cells primarily catabolize glucose to carbon dioxide by oxidative phosphorylation. On the other hand, cancer cells 'ferment' glucose into lactate (glycolysis) even when access to sufficient oxygen is available. This phenomenon is known as aerobic glycolysis or the Warburg effect [57]. It is becoming more evident that actively proliferating cells consume glucose not only for ATP production, but also for the synthesis of nucleotides or fatty acids [58]. TALDO1 and G6PD are critical enzymes in the glycolysis shunt, the pentose phosphate pathway. ALDOA is an enzyme for mainstream glycolysis. It has been reported that the expression of ALDOA mRNA is increased in cancer cells in HCCs [59], thus fitting the conventional concept of enhanced glycolysis. Consistently, the expressions of ALDOA and G6PD in the present study were both upregulated, which suggested enhanced glycolysis and was hypothesized to be due to cell proliferation induced by PFOA.

In summary, our study showed novel sight into the liver toxicity of PFOA on human cells. Low doses of PFOA stimulated cell proliferation by promoting cells transition from the G1 to S phase to increase cell numbers, whereas high doses of PFOA (200–400 μM) led to a reduced number of HL-7702 cells compared with the control, which was likely due to cell cycle arrest in the G0/G1 phase. Additionally, cell arrest in the G0/G1 phase might be attributed to the p53-independent pathway. To our knowledge, this is the first report on PFOA promotion of cell cycle progression in human cells. We hope this study can provide novel insight to evaluate the risk of PFAAs to human health after long-term and constant exposure at low environmental concentrations.

Acknowledgements

This work was supported by the Strategic Priority Research Program of the Chinese Academy of Sciences (XDB14040202) and the National Natural Science Foundation of China (grant Nos. 31320103915 and 21277143).

Appendix A. Supplementary data

Supplementary data associated with this article can be found, in the online version, at http://dx.doi.org/10.1016/j.jhazmat.2016.03.077.

References

[1] 3M, 3M The Leader in Electrofluorination, 3M Company Technical Bulletin, 3M company, St. Paul, MN, 1995.
[2] M. Houde, J.W. Martin, R.J. Letcher, K.R. Solomon, D.C. Muir, Biological monitoring of polyfluoroalkyl substances: a review, Environ. Sci. Technol. 40 (2006) 3463–3473.
[3] J.P. Giesy, K. Kannan, Perfluorochemical surfactants in the environment, Environ. Sci. Technol. 36 (2002) 146A–152A.
[4] A. Rotander, A. Karrman, B. van Bavel, A. Polder, F. Riget, G.A. Auethunsson, G. Vikingsson, G.W. Gabrielsen, D. Bloch, M. Dam, Increasing levels of long-chain perfluorocarboxylic acids (PFCAs) in Arctic and North Atlantic marine mammals, 1984–2009, Chemosphere 86 (2012) 278–285.
[5] A.L. Brantsaeter, K.W. Whitworth, T.A. Ydersbond, L.S. Haug, M. Haugen, H.K. Knutsen, C. Thomsen, H.M. Meltzer, G. Becher, A. Sabaredzovic, J.A. Hoppin, M. Eggesbo, M.P. Longnecker, Determinants of plasma concentrations of perfluoroalkyl substances in pregnant Norwegian women, Environ. Int. 54 (2013) 74–84.
[6] C. Lau, K. Anitole, C. Hodes, D. Lai, A. Pfahles-Hutchens, J. Seed, Perfluoroalkyl acids: a review of monitoring and toxicological findings, Toxicol. Sci. 99 (2007) 366–394.
[7] S.J. Frisbee, A.P. Brooks Jr., A. Maher, P. Flensborg, S. Arnold, T. Fletcher, K. Steenland, A. Shankar, S.S. Knox, C. Pollard, J.A. Halverson, V.M. Vieira, C. Jin, K.M. Leyden, A.M. Ducatman, The C8 health project: design, methods, and participants, Environ. Health Perspect. 117 (2009) 1873–1882.
[8] J.A. Gleason, G.B. Post, J.A. Fagliano, Associations of perfluorinated chemical serum concentrations and biomarkers of liver function and uric acid in the US population (NHANES), 2007–2010, Environ. Res. 136 (2015) 8–14.
[9] A.M. Calafat, Z. Kuklenyik, J.A. Reidy, S.P. Caudill, J.S. Tully, L.L. Needham, Serum concentrations of 11 polyfluoroalkyl compounds in the u.s. population: data from the national health and nutrition examination survey (NHANES), Environ. Sci. Technol. 41 (2007) 2237–2242.
[10] G.W. Olsen, J.M. Burris, M.M. Burlew, J.H. Mandel, Plasma cholecystokinin and hepatic enzymes, cholesterol and lipoproteins in ammonium perfluorooctanoate production workers, Drug Chem. Toxicol. 23 (2000) 603–620.
[11] G.L. Kennedy Jr., J.L. Butenhoff, G.W. Olsen, J.C. O'Connor, A.M. Seacat, R.G. Perkins, L.B. Biegel, S.R. Murphy, D.G. Farrar, The toxicology of perfluorooctanoate, Crit. Rev. Toxicol. 34 (2004) 351–384.
[12] C. Lau, J.L. Butenhoff, J.M. Rogers, The developmental toxicity of perfluoroalkyl acids and their derivatives, Toxicol. Appl. Pharmacol. 198 (2004) 231–241.
[13] J.C. DeWitt, M.M. Peden-Adams, J.M. Keller, D.R. Germolec, Immunotoxicity of perfluorinated compounds: recent developments, Toxicol. Pathol. 40 (2012) 300–311.
[14] S.G. Hundley, A.M. Sarrif, G.L. Kennedy, Absorption, distribution, and excretion of ammonium perfluorooctanoate (APFO) after oral administration to various species, Drug Chem. Toxicol 29 (2006) 137–145.
[15] C.R. Elcombe, B.M. Elcombe, J.R. Foster, S.C. Chang, D.J. Ehresman, J.L. Butenhoff, Hepatocellular hypertrophy and cell proliferation in Sprague-Dawley rats from dietary exposure to potassium perfluorooctanesulfonate results from increased expression of xenosensor nuclear receptors PPARalpha and CAR/PXR, Toxicology 293 (2012) 16–29.
[16] M. Minata, K.H. Harada, A. Karrman, T. Hitomi, M. Hirosawa, M. Murata, F.J. Gonzalez, A. Koizumi, Role of peroxisome proliferator-activated receptor-alpha in hepatobiliary injury induced by ammonium perfluorooctanoate in mouse liver, Ind. Health 48 (2010) 96–107.
[17] M.B. Rosen, B.D. Abbott, D.C. Wolf, J.C. Corton, C.R. Wood, J.E. Schmid, K.P. Das, R.D. Zehr, E.T. Blair, C. Lau, Gene profiling in the livers of wild-type and PPARalpha-null mice exposed to perfluorooctanoic acid, Toxicol. Pathol. 36 (2008) 592–607.
[18] M.B. Rosen, J.S. Lee, H. Ren, B. Vallanat, J. Liu, M.P. Waalkes, B.D. Abbott, C. Lau, J.C. Corton, Toxicogenomic dissection of the perfluorooctanoic acid transcript profile in mouse liver: evidence for the involvement of nuclear receptors PPAR alpha and CAR, Toxicol. Sci. 103 (2008) 46–56.
[19] T. Panaretakis, I.G. Shabalina, D. Grander, M.C. Shoshan, J.W. DePierre, Reactive oxygen species and mitochondria mediate the induction of apoptosis in human hepatoma HepG2 cells by the rodent peroxisome proliferator and hepatocarcinogen, perfluorooctanoic acid, Toxicol. Appl. Pharmacol. 173 (2001) 56–64.
[20] E. Scharmach, T. Buhrke, D. Lichtenstein, A. Lampen, Perfluorooctanoic acid affects the activity of the hepatocyte nuclear factor 4 alpha (HNF4alpha), Toxicol. Lett. 212 (2012) 106–112.
[21] I.G. Shabalina, T. Panaretakis, A. Bergstrand, J.W. DePierre, Effects of the rodent peroxisome proliferator and hepatocarcinogen perfluorooctanoic acid, on apoptosis in human hepatoma HepG2 cells, Carcinogenesis 20 (1999) 2237–2246.
[22] M. Tian, S. Peng, F.L. Martin, J. Zhang, L. Liu, Z. Wang, S. Dong, H. Shen, Perfluorooctanoic acid induces gene promoter hypermethylation of glutathione-*S*-transferase Pi in human liver L02 cells, Toxicology 296 (2012) 48–55.
[23] C.Y. Lin, L.Y. Lin, C.K. Chiang, W.J. Wang, Y.N. Su, K.Y. Hung, P.C. Chen, Investigation of the associations between low-dose serum perfluorinated chemicals and liver enzymes in US adults, Am. J. Gastroenterol. 105 (2010) 1354–1363.
[24] V. Gallo, G. Leonardi, B. Genser, M.J. Lopez-Espinosa, S.J. Frisbee, L. Karlsson, A.M. Ducatman, T. Fletcher, Serum perfluorooctanoate (PFOA) and

perfluorooctane sulfonate (PFOS) concentrations and liver function biomarkers in a population with elevated PFOA exposure, Environ. Health Perspect. 120 (2012) 655–660.
[25] G. Costa, S. Sartori, D. Consonni, Thirty years of medical surveillance in perfluooctanoic acid production workers, J. Occup. Environ. Med. 51 (2009) 364–372.
[26] M.B. Rosen, C. Lau, J.C. Corton, Does exposure to perfluoroalkyl acids present a risk to human health? Toxicol. Sci. 111 (2009) 1–3.
[27] G.A. Bounda, W. Zhou, D.D. Wang, F. Yu, Rhein elicits in vitro cytotoxicity in primary human liver hl-7702cells by inducing apoptosis through mitochondria-mediated pathway, Evid. Based Complement. Altern. Med. 2015 (2015) 329831.
[28] H. Zhang, Y. Lu, B. Luo, S. Yan, X. Guo, J. Dai, Proteomic analysis of mouse testis reveals perfluorooctanoic acid-induced reproductive dysfunction via direct disturbance of testicular steroidogenic machinery, J. Proteome Res. 13 (2014) 3370–3385.
[29] N.A. Karp, W. Huber, P.G. Sadowski, P.D. Charles, S.V. Hester, K.S. Lilley, Addressing accuracy and precision issues in iTRAQ quantitation, Mol. Cell. Proteomics 9 (2010) 1885–1897.
[30] K. Lohr, C. Moritz, A. Contente, M. Dobbelstein, p21/CDKN1A mediates negative regulation of transcription by p53, J. Biol. Chem. 278 (2003) 32507–32516.
[31] I.A. Atencio, M. Ramachandra, P. Shabram, G.W. Demers, Calpain inhibitor 1 activates p53-dependent apoptosis in tumor cell lines, Cell Growth Differ. 11 (2000) 247–253.
[32] G.W. Porter, F.R. Khuri, H. Fu, Dynamic 14-3-3/client protein interactions integrate survival and apoptotic pathways, Semin. Cancer Biol. 16 (2006) 193–202.
[33] D.Z. Fu, Y. Cheng, H. He, H.Y. Liu, Y.F. Liu, PDCD5 expression predicts a favorable outcome in patients with hepatocellular carcinoma, Int. J. Oncol. 43 (2013) 821–830.
[34] M. Spinola, P. Meyer, S. Kammerer, F.S. Falvella, M.B. Boettger, C.R. Hoyal, C. Pignatiello, R. Fischer, R.B. Roth, U. Pastorino, K. Haeussinger, M.R. Nelson, R. Dierkesmann, T.A. Dragani, A. Braun, Association of the PDCD5 locus with lung cancer risk and prognosis in smokers, J. Clin. Oncol. 24 (2006) 1672–1678.
[35] Y.H. Yang, M. Zhao, W.M. Li, Y.Y. Lu, Y.Y. Chen, B. Kang, Y.Y. Lu, Expression of programmed cell death 5 gene involves in regulation of apoptosis in gastric tumor cells, Apoptosis 11 (2006) 993–1001.
[36] J. Sudbo, A. Reith, O.C. Lingjaerde, Gene-expression profiles in hereditary breast cancer, N. Engl. J. Med 344 (2001) 2029.
[37] X. Zhang, X. Wang, X. Song, Z. Wei, C. Zhou, F. Zhu, Q. Wang, C. Ma, L. Zhang, Clinical and prognostic significance of lost or decreased PDCD5 expression in human epithelial ovarian carcinomas, Oncol. Rep. 25 (2011) 353–358.
[38] L.N. Chen, Y. Wang, D.L. Ma, Y.Y. Chen, Short interfering RNA against the PDCD5 attenuates cell apoptosis and caspase-3 activity induced by Bax overexpression, Apoptosis 11 (2006) 101–111.
[39] X.Z. Hu, D.C. Hu, Effects of perfluorooctanoate and perfluorooctane sulfonate exposure on hepatoma Hep G2 cells, Arch. Toxicol. 83 (2009) 851–861.
[40] P. Fernandez Freire, J.M. Perez Martin, O. Herrero, A. Peropadre, E. de la Pena, M.J. Hazen, In vitro assessment of the cytotoxic and mutagenic potential of perfluorooctanoic acid, Toxicol. In Vitro 22 (2008) 1228–1233.
[41] Q. Huang, J. Zhang, F.L. Martin, S. Peng, M. Tian, X. Mu, H. Shen, Perfluorooctanoic acid induces apoptosis through the p53-dependent mitochondrial pathway in human hepatic cells: a proteomic study, Toxicol. Lett. 223 (2013) 211–220.
[42] M. Molinari, Cell cycle checkpoints and their inactivation in human cancer, Cell Prolif. 33 (2000) 261–274.
[43] M.V. Blagosklonny, A.B. Pardee, The restriction point of the cell cycle, Cell Cycle 1 (2014) 102–109.
[44] E. Lees, B. Faha, V. Dulic, S.I. Reed, E. Harlow, Cyclin E/cdk2 and cyclin A/cdk2 kinases associate with p107 and E2F in a temporally distinct manner, Genes Dev. 6 (1992) 1874–1885.
[45] K. Katayama, N. Fujita, T. Tsuruo, Akt/protein kinase B-dependent phosphorylation and inactivation of WEE1Hu promote cell cycle progression at G2/M transition, Mol. Cell. Biol. 25 (2005) 5725–5737.
[46] C.J. Rothblum-Oviatt, C.E. Ryan, H. Piwnica-Worms, 14-3-3 binding regulates catalytic activity of human Wee1 kinase, Cell Growth Differ. 12 (2001) 581–589.
[47] T.A. Chan, P.M. Hwang, H. Hermeking, K.W. Kinzler, B. Vogelstein, Cooperative effects of genes controlling the G(2)/M checkpoint, Genes Dev. 14 (2000) 1584–1588.
[48] Z.N. Oltvai, C.L. Milliman, S.J. Korsmeyer, Bcl-2 heterodimerizes in vivo with a conserved homolog, bax, that accelerates programmed cell death, Cell 74 (1993) 609–619.
[49] J.E. Klaunig, B.A. Hocevar, L.M. Kamendulis, Mode of action analysis of perfluorooctanoic acid (PFOA) tumorigenicity and human relevance, Reprod. Toxicol. 33 (2012) 410–418.
[50] J.A. Bjork, J.L. Butenhoff, K.B. Wallace, Multiplicity of nuclear receptor activation by PFOA and PFOS in primary human and rodent hepatocytes, Toxicology 288 (2011) 8–17.
[51] D.C. Wolf, T. Moore, B.D. Abbott, M.B. Rosen, K.P. Das, R.D. Zehr, A.B. Lindstrom, M.J. Strynar, C. Lau, Comparative hepatic effects of perfluorooctanoic acid and WY 14,643 in PPAR-alpha knockout and wild-type mice, Toxicol. Pathol. 36 (2008) 632–639.
[52] J.H. Teruya, S.Y. Kutsunai, D.H. Spear, P.A. Edwards, C.F. Clarke, Testis-specific transcription initiation sites of rat farnesyl pyrophosphate synthetase mRNA, Mol. Cell. Biol. 10 (1990) 2315–2326.
[53] N. Kudo, Y. Kawashima, Fish oil-feeding prevents perfluorooctanoic acid-induced fatty liver in mice, Toxicol. Appl. Pharmacol. 145 (1997) 285–293.
[54] S. Yan, J. Wang, J. Dai, Activation of sterol regulatory element-binding proteins in mice exposed to perfluorooctanoic acid for 28 days, Arch. Toxicol. 89 (2015) 1569–1578.
[55] J.D. Horton, J.L. Goldstein, M.S. Brown, SREBPs: activators of the complete program of cholesterol and fatty acid synthesis in the liver, J. Clin. Invest. 109 (2002) 1125–1131.
[56] S.M. Jackson, J. Ericsson, R. Mantovani, P.A. Edwards, Synergistic activation of transcription by nuclear factor Y and sterol regulatory element binding protein, J. Lipid Res. 39 (1998) 767–776.
[57] O. Warburg, On the origin of cancer cells, Science 123 (1956) 309–314.
[58] M.G. Vander Heiden, L.C. Cantley, C.B. Thompson, Understanding the Warburg effect: the metabolic requirements of cell proliferation, Science 324 (2009) 1029–1033.
[59] G. Castaldo, G. Calcagno, R. Sibillo, R. Cuomo, G. Nardone, L. Castellano, C. Del Vecchio Blanco, G. Budillon, F. Salvatore, Quantitative analysis of aldolase A mRNA in liver discriminates between hepatocellular carcinoma and cirrhosis, Clin. Chem. 46 (2000) 901–906.